sciendo

Slovak Journal of Civil Engineering

Vol. 32, 2024, No. 1, 36 – 45
DOI: 10.2478/sjce-2024-0005

CALIBRATION OF HYPOPLASTIC PARAMETERS FOR DANUBE SAND

Amir Mosallaei[1]*, András Mahler[1]

Abstract

The relationship between stress and strain tensors in soil is described by the soil constitutive equation, which depends on the soil type and deformation conditions. The development of various constitutive models has enabled a better understanding of the macromechanical properties of soil. One such model is hypoplasticity, which was discovered more than three decades ago. The purpose of this study is to determine whether hypoplasticity could accurately represent the behavior of Danube sand, a specific type of sand. The researchers conducted laboratory measurements to obtain the eight basic hypoplastic parameters of Danube sand and employed the intergranular strain concept as an extension of hypoplasticity to achieve a more precise material behavior. All the parameters were then utilized to simulate the cyclic triaxial test using the SoilTest Module of PLAXIS. The results showed that the hypoplastic constitutive simulation model for Danube sand was capable of making relatively accurate predictions for accumulative settlement.

Address

[1] Dept. of Engineering Geology and Geotechnics, Budapest University of Technology and Economics, Budapest, Hungary

* ***Corresponding author:*** mosallaei@edu.bme.hu

Key words

- Hypoplasticity,
- Intergranular strain,
- Cyclic triaxial test,
- Coarse-grained soil,
- Constitutive model.

1 INTRODUCTION

In recent decades, various numerical techniques have been developed to model soil behavior under static and cyclic loads. A suitable constitutive model must be used to effectively depict the interaction between soil and structures, especially in the case of geotechnical structures on water-saturated soils subjected to cyclic stress. The Mohr-Coulomb frictional constitutive model is often used, but it fails to account for the complex historical dependence of soil behavior. Therefore, more advanced models, such as the hypoplastic constitutive model with a critical state, have been proposed. The calibration of these models requires high-quality cyclic laboratory tests with a variety of boundary conditions (Gajári et al., 2021; Niemunis et al., 2005; Stutz et al., 2017a; Wei and Yang, 2020; Wichtmann and Triantafyllidis, 2018; Wu et al., 2017).

In this paper, the hypoplasticity parameters of Danube sand are calibrated to obtain an accurate set of soil properties for simulating pavement-subsoil interactions. It is important to consider the accumulation of cyclic traffic loads and residual stresses, which can cause tensile cracks in asphalt. Moreover, cyclic loading can cause irreversible strains and excessive pore pressure, leading to soil liquefaction and loss of overall stability. Therefore, the accumulation strain phenomenon is of practical importance.

1.1 Hypoplasticity and its basis

By defining the relationship between stress and strain through mathematical equations, constitutive laws are responsible for describing how materials deform. Various mathematical equations have been developed to describe the deformation behavior of soil. Hypoplastic equations,

© 2024 The Author(s). This is an open access article licensed under the Creative Commons Attribution 4 .0 License (https://creativecommons.org/licenses/by/4.0/)

which are based on non-linear tensor functions, have proven to be particularly useful for modeling granular soils (von Wolffersdorff, 1996). Unlike plasticity-based equations, hypoplastic equations do not rely on yield surfaces or the decomposition of a strain into elastic and plastic components, thereby resulting in simpler initial formulations with fewer parameters. These equations can also account for the effects of pressure and density changes and can be validated through laboratory tests. Over time, hypoplastic equations have been improved to include additional state variables, such as porosity, and can be determined through lab tests. The stress tensor is the only state variable in the basic hypoplastic equations (Bauer et al., 2020; Fellin, 2002; Wang and Wu, 2020).

Initially, the hypoplastic state equation only considered the stress tensor as a variable, and the basic hypoplastic equations included four polynomial expressions, four material characteristic coefficients, two linear coefficients, and two nonlinear coefficients to describe the strain rate. Over time, improvements were made to hypoplastic equations by adding a new state variable, i.e., porosity. The advantage of hypoplastic equations is that the main parameters can be obtained through triaxial equipment. The stress tensor remains the only state variable in the basic hypoplastic equations (Wu et al., 2017).

The hypoplastic behavior model has been extensively used to study the behavior of sandy soils and has been shown to accurately express uniform settlement. It can even be used for soft soils with a high internal friction angle. However, when using the hypoplastic behavior model for clay soils, the stiffness of the modeled soil is much lower than in reality (Herle and Kolymbas, 2004).

The hypoplastic model correctly predicts the arrangement of the grain skeleton causing sediment deformation, density, and pressure using material constants and a simple formula. However, without an intergranular strain (IS) parameter, it cannot predict soil behavior in certain cases, such as the soil‘s initial high degree of stiffness and cumulative plastic deformations generated by small stress loading cycles (Herle and Gudehus, 1999; Kolymbas and Wu, 1990; Mohammadi-Haji and Ardakani, 2020).

Model parameters for granular materials should directly depend on grain properties, such as shape, angularity, size distribution, and the friction coefficient, as well as the grain’s hardness or strength. However, determining these parameters from experimental investigations of single grains is not realistic (Herle and Gudehus, 1999).

2 METHODS ANDS PARAMETERS

The behavior of granular soils under a load is primarily determined by their stress level. As a confining pressure increases, the maximum shear strength of granular soils typically increases, while residual shear strength and stiffness may also increase or remain relatively constant, depending on the specific material properties and conditions. Cumulative deformation is a major concern for the long-term serviceability of structures susceptible to differential defor-mation. “Hypoplasticity” is a model used to describe the behavior of sand, which does not require a yield surface or other elements related to elastoplasticity. Wu and Bauer (1994) proposed a four-parameter model that could describe various characteristics of sand in both drained and undrained states. Niemunis and Herle (1997) presented the formulation of small strain stiffness, while Poblete et al., (2016) proposed the framework of intergranular strain anisotropy (ISA), which allows for improved model performance under cyclic loading conditions, such as memory effects and increased stiffness upon stress reversal (Mohammadi-Haji and Ardakani, 2020; Moussa et al., 2020; Yang et al., 2020).

2.1 Basic parameters

The hypoplastic model for sand is comprised of eight parameters, which can be divided into

four major categories. The first category pertains to the critical friction angle, denoted as φ_c.

The second category includes two parameters, i.e., h_s, which stands for granular stiffness, and n, which serves as an exponent for h_s. The third category is dedicated to various types of void ratios, where e_{d0} represents the minimum void ratio at zero pressure; e_{c0} represents the critical void ratio at zero pressure; and e_{i0} represents the maximum void ratio at zero pressure. The fourth and final category encompasses the last two parameters, α and β, which respectively impact the peak of the friction angle and control the stiffness. Wolffersdorff‘s hypoplastic model is used in this paper (von Wolffersdorff, 1996).

2.1.1 Friction Angle φ_c of the Critical State

The parameter φ_c represents the critical angle of internal friction, which is a fundamental parameter in soil mechanics and geotechnical engineering. It describes the minimum angle at which a soil mass will fail or slide under shear stress and determines the soil‘s shear strength. The critical friction angle varies, depending on the soil type and state of stress and can be determined through laboratory and field tests.

Herle and Gudehus (1999) showed that the angle of repose measured on a dry granular soil provides a good estimate of the critical friction angle determined through shear box measurements.

In coarse-grained soils, the angle of repose test is a straightforward method for determining φ_c. However, for soils with a larger proportion of fine grains, triaxial shear tests on normally consolidated samples are recommended.

Soil, typically reaches its critical state under monotonic shear loading when the volumetric deformation rate stabilizes while maintaining a constant mean stress. Triaxial tests are commonly used to determine the critical state.

Tab. 1 *Critical friction angle from angles of repose and from shear tests (Herle and Gudehus, 1999)*

Material	Hochstetten gravel	Hochstetten sand	Hostun sand	Karlsruhe sand	Lausitz sand	Toyoura sand	Zbraslav sand
Angle of repose	35.7	34	32	29.1	33	30.4	30.8
φ_c	36.5	34	32	30	32.2	30.9	29.7

2.1.2 Granulate Hardness (h_s) and exponent (n)

The term „granulate hardness“ refers to the extent of resistance or firmness displayed by granular materials when subjected to an applied force or load. The measurement of granulate hardness is valuable for gathering information on the particle size distribution, packing density, and flow characteristics of the material, which can aid in optimizing handling and processing operations. Various techniques, such as penetrometers, compressive testing, and shear testing, are available for measuring granulate hardness.

Granular hardness (h_s) is the only parameter that measures stress and should not be confused with the hardness of individual grains. The exponent „n“ accounts for the pressure-sensitivity of the grain skeleton, allowing for a non-proportional increase in incremental stiffness with increasing pressure. An oedometer test is a simpler way of determining “h_s” and “n”. Directly obtaining “h_s” and “n” from measured data is not recommended due to strong non-linearity. The knowledge of “n” is necessary for determining “h_s”, but “n” can be calculated independently of “h_s”. An oedometric test can replace isotropic compression for calibration asit is easier to perform and allows for reaching higher pressure, as “h_s” and “n” control the slope and curvature of the compression line, respectively.

Performing an oedometer test and plotting the compression curve yields a graph similar to Figure 1, which represents a schematic of the compression curve. The calculation of the exponent „n“ is the first step, as it is not dependent on the parameter „h_s,“ which is absent in Equation 1. The determination of „n“ is crucial in determining „h_s,“ which can be calculated using Equation 2. Thus, the value of „h_s“ depends on knowledge of „n.“

$$n = \frac{\ln\left(\frac{e_{p1}\times c_{c2}}{e_{p2}\times c_{c1}}\right)}{\ln\left(\frac{p_{s2}}{p_{s1}}\right)} \tag{1}$$

$$h_s = 3 \times p \times \left(\frac{n\times e}{c_c}\right)^{\frac{1}{n}} \tag{2}$$

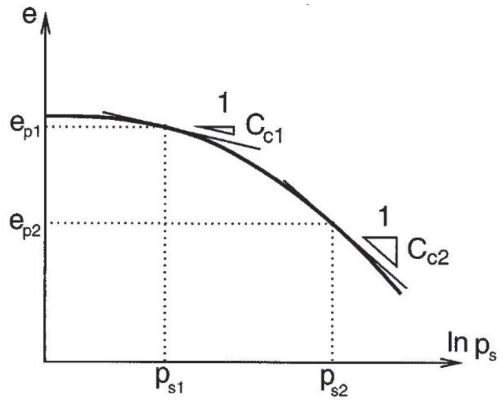


Fig. 1 *Schematic of compression curve (Herle and Gudehus, 1999)*

2.1.3 Minimum e_{d0}, critical e_{c0}, and maximum e_{i0} of a void ratio at zero pressure

Generally, the most effective way to achieve the optimal compaction of a granular soil is by applying cyclic shearing with a small amplitude under constant pressure. When this technique is implemented following static compression, it will gradually approach a minimum void ratio e_d, which decreases with increasing pressure. Equation 3 below can be used to describe the relationship between e_d and p_s, enabling the extrapolation of the value of e_d at zero pressure.

$$\boldsymbol{e_{d0} = e_d\, exp\left[\left(\frac{3p_s}{h_s}\right)^n\right]} \tag{3}$$

Typically, a minimum void ratio (e_{min}) is determined using index tests outlined in several standards. However, these tests are not as efficient as cyclic shearing. As a result, the measured value of e_{min} may be higher than that of e_d. Upon comparing e_{d0} with e_{min}, it is determined that they are relatively similar, with e_{min} being slightly higher than e_{d0}. Therefore, in the absence of data for e_{d0}, e_{min} can be used as a substitute (Herle and Gudehus, 1999).

Similarly to e_{d0}, the critical void ratio value at zero pressure can be computed using equation 4 below:

$$\boldsymbol{e_{c0} = e_c\, exp\left[\left(\frac{3p_s}{h_s}\right)^n\right]} \tag{4}$$

The parameter e_c can be determined through a shear test on a soil element while calculating φ_c. An undrained triaxial test is usually sufficient for establishing e_c. It has been noted that the value of e_{c0} is comparable to e_{max}.

Previously, Herle and Gudehus (1999) indicated a narrow range of 0.52 to 0.64 for the ratio of e_{d0}/e_{c0}. Mašín (2019) also proposed an empirical formula of e_{d0}=0.5*e_{c0} to be used when experimental data is not available. Tables 2 and 3 include 39 sets of hypoplastic parameters obtained from previous investigations. Based on Tables 2 and 3, the range for the aforementioned ratio is 0.37 to 0.77, with an average ratio of 0.56, which is very similar to the earlier empirical formula.

The parameter e_{i0} represents the highest possible void ratio of a basic grain skeleton achieved during an isotropic consolidation of a grain suspension in an environment without gravity. There are several ways to determine the maximum void ratio e_{max} in the laboratory, with most standards involving pouring dry soil into a calibrated mold. However, the soil often reaches a critical state during pouring, which is denser than the theoretical e_{max}. While the maximum void ratio in a gravity-free space is proposed, it cannot be measured in a laboratory. Herle and Gudehus (1999) discovered that for spherical grains, this value is 1.2 times the emax, while for cube grains, it is 1.3 times the e_{max}.

By examining Tables 2 and 3, it can be observed that the ratio of e_{i0} to e_{c0} is generally less than 1.3, and sometimes even less than 1.2. The average value for this parameter is 1.14.

2.1.4 Exponents α and β

The stiffness and pyknotropy factors are controlled by parameters α and β, which can be determined through a parametric study involving simulations of the triaxial shear test. To obtain α, Herle and Gudehus (1999) suggested using equation (2) and considering the peak state in a triaxial compression test.

$$\alpha = \frac{\ln\left[6\times\frac{(2+K_P)^2+a^2K_P(K_P-1-\tan\nu_P)}{a(2+K_P)(5K_P-2)\sqrt{4+2(1+\tan\nu_P)^2}}\right]}{\ln\frac{e-e_d}{e_c-e_d}} \tag{6}$$

Equation 6 above involves K_p, a and tan(ν_p), which can be calculated using equations 7, 8, and 9 below, respectively.

$$K_P = \frac{1+\sin\varphi_P}{1-\sin\varphi_P} \quad (7)$$

$$a = \frac{\sqrt{3}(3-\sin\varphi_c)}{2\sqrt{2}\sin\varphi_c} \quad (8)$$

$$\tan\nu_P = 2\frac{K_P-4+5AK_P{}^2-2AK_P}{(5K_P-2)(1+2A)} - 1 \quad (9)$$

To determine tan(ν_P), equation 10 can be used to calculate parameter A. An evaluation of α and β requires knowledge of these preceding parameters.

$$A = \frac{a^2}{(2+K_P)^2}\left[1 - \frac{K_p(4-K_P)}{5K_P-2}\right] \quad (10)$$

The parameter β is significant only when the void ratio e is significantly lower than the initial void ratio e_i. According to Herle and Gudehus (1999), for natural sands, assuming β = 1 is usually adequate, regardless of granulometric properties. However, among the 38 data sets in Tables 2 and 3, it can be observed that only 10 out of 38 have a value of 1 for β, while the β parameter for the remaining sets is greater than 1.

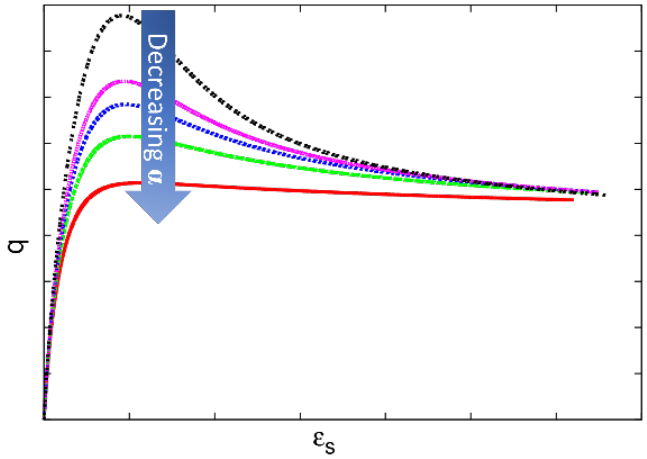


Fig. 2 *Effect of α on the peak of a stress- strain curve (Mašín, 2015)*

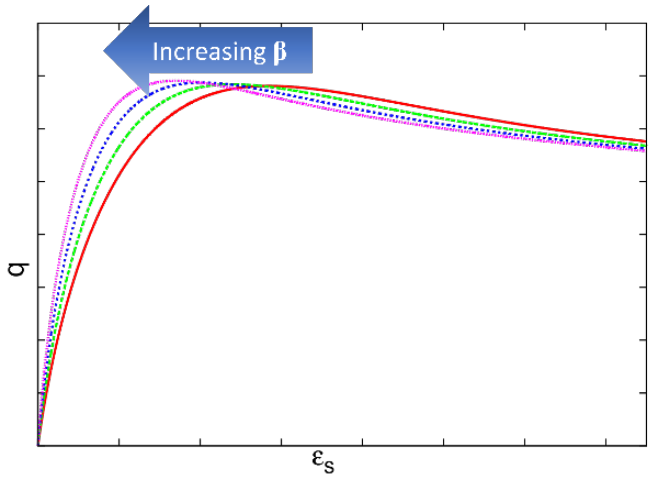


Fig. 3 *Effect of β on the peak of a stress-strain curve (Mašín, 2015)*

The impact of the α and β parameters on stress-strain curves can be understood through Figures 2 and 3. A drained triaxial test on a dense sample and curve simulation using various amounts of α can be conducted to calibrate these parameters. Fitting the resulting curves will yield the optimal value for α. Figure 2 shows that increasing α decreases the stress peak on the stress- strain curve, while Figure 3 shows β changes the location of the peak by reducing the strain value and shifting the peak to the left.

2.2 Intergranular strain parameters

Basic hypoplastic models are inadequate in predicting high initial stiffness and ratcheting, which is the accumulation of strains in stress cycles and stresses in strain cycles. The intergranular strain concept is the most widely-used approach for overcoming this limitation (Niemunis and Herle, 1997). The ISA theory provides a useful mathematical platform for developing constitutive models to simulate cyclic loading in soils by considering the effect of recent strain history. The intergranular strain evolution equation is elasto-plastic and based on a simple bounding surface approach. The concept assumes that the reversible deformation of the intergranular strain layer, combined with the elastic deformation of the grains, accounts for all the measured soil deformations at the beginning of the loading process until a certain amount of strain is reached, and the grains start to rearrange. This reversible deformation is described by an additional component of the model, while the deformation associated with the grain rearrangement is irreversible and predicted by the standard hypo-plastic model. Introducing the intergranular strain adds five more parameters, namely, m_R, m_T, β_r, R, and χ to the basic parameters; they are discussed in detail in the following sections (Yang et al., 2020). Niemunis' IS model is used for this investigation (Niemunis et al., 2005).

2.2.1 Stiffness factor (m_R)

The m_R parameter has a crucial role in regulating the shear modulus strength at extremely low strain values, whether it is during initial loading or when the strain path direction is reversed by 180 degrees. The most precise approach for ascertaining the value of m_R is via shear wave propagation experiments such as bender element tests. Although static shear tests can also measure the shear modulus, this method is less dependable as it relies on local measurements of sample deformations, and strain transducers have limitations regarding their accuracy.

2.2.2 Parameter m_T

Determining the m_T parameter (or m_{rat} ratio = m_T / m_R) through experimentation is a difficult task. The m_{rat} value indicates the ratio of the initial shear stiffness (G_0) to the shear stiffness after a 90-degree change in the strain path direction (G_{90}), expressed as G_{90}/G_0. Measuring G_{90} requires precise local strain transducers as it cannot be measured through wave propagationtechniques. To make it more convenient, Mašín (2019) recommends a default value of 0.7 for m_{rat} if there is no experimental data available for the soil of interest.

Figure 5 illustrates the relationship between m_R and m_T based on 14 sets of data collected in Tables 2 and 3. Therefore, in the absence of experimental data for m_T, according to Figure 4, a value of m_T=0.5*m_R can be used.

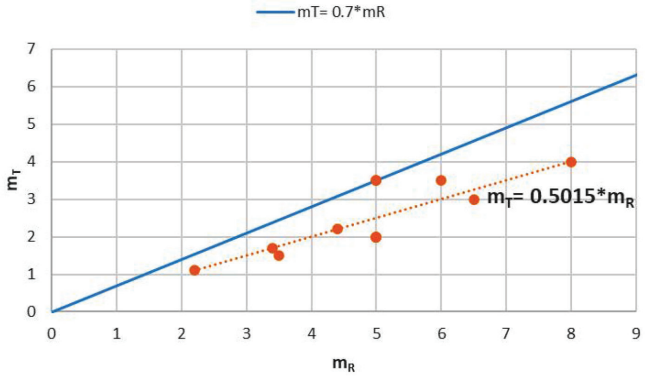


Fig. 4 *Relation between m_T and m_R*

2.2.3 Elastic strain amplitude, Intergranular strain hardening parameter and exponent

The intergranular strain concept model utilizes three parameters, namely R, β_r, and χ, each with a distinct physical interpretation. The parameter R specifies the extent of the elastic range in the strain space, whereas β_r controls the rate of evolution of the intergranular strain tensor. On the other hand, χ regulates the interpolation between the reversible elastic and nonlinear hypoplastic response. Despite their varied interpretations, these parameters work together to determine the rate of stiffness degradation with increasing strains, which, in turn, affect the predictions of the model. The calibration of these parameters usually involves triaxial shear experiments, which measure local deformations, and obtains shear moduli versus shear strain curves. An increase in R causes a decrease in βr and shifts the stiffness degradation curve horizontally in the G versus ln(ε_s) diagram. Conversely, χ influences the rate of a decrease in stiffness with a strain, and a higher χ value leads to a larger quasi-elastic range size and a faster subsequent rate of decrease in stiffness. To calibrate the χ parameter, an experimental trial-and- error process is required to fit the data.

Tab. 2 *Basic hypoplastic parameters of different types of soil*

	Basic hypoplastic							
	φ_c (°)	h_s (MPa)	n	e_{d0}	e_{c0}	e_{i0}	α	β
Hochstetten gravel (Herle and Gudehus, 1999)	36	3.2000E+04	0.18	0.26	0.45	0.5	0.1	1.9
Hochstetten sand (Herle and Gudehus, 1999)	33	1.5000E+03	0.28	0.55	0.95	1.5	0.25	1
Hochstetten sand (A. Niemunis and Herle, 1997)	33	1.0000E+03	0.25	0.55	0.95	1.5	0.25	1
Hostun sand (Herle and Gudehus, 1999)	31	1.0000E+03	0.29	0.61	0.96	1.9	0.13	2
Karlsruhe sand (Herle and Gudehus, 1999)	30	5.8000E+03	0.28	0.53	0.84	1	0.13	1
Lausitz sand (Herle and Gudehus, 1999)	33	1.6000E+03	0.19	0.44	0.85	1	0.25	1
Toyoura sand (Herle and Gudehus, 1999)	30	2.6000E+03	0.27	0.61	0.98	1.1	0.18	1.1
Zbraslav sand (Herle and Gudehus, 1999)	31	5.7000E+03	0.25	0.52	0.82	0.95	0.13	1
Uncemented gravel (Fu et al., 2021)	39.5	7.5000E+01	0.55	0.17	0.40	0.48	0.06	1.5
Uncemented sand (Fu et al., 2021)	28.6	9.5500E+01	0.45	0.48	0.75	0.86	0.15	1.25
Karlsruhe fine sand (Poblete et al., 2016)	33	8.6260E+01	0.32	0.67	1.9	1.21	0.21	1.5
Karlsruhe fine sand (Fuentes et al., 2020)	32.6	4.0000E+03	0.27	0.677	1.054	1.212	0.14	2.5
Prague sand (Kadlíček et al., 2016)	35.47	9.0530E+01	0.56	0.33	0.66	0.79	0.03	1.9
Komorany sand (Mašín, 2019)	35	5.0000E+01	0.2	0.35	0.87	1.4	0.26	4
Dobrany (Kadlíček et al., 2022)	41.1	6.5339E+01	0.207	0.592	1.183	1.42	0.05	4
Hrusovany (Kadlíček et al., 2022)	42.6	1.9030E+00	0.162	0.591	1.182	1.418	0.07	6.3
Jablonec (Kadlíček et al., 2022)	42.6	1.0370E+00	0.232	0.616	1.232	1.478	0.02	4.1
Kralupy (Kadlíček et al., 2022)	41.2	1.7560E+00	0.149	0.809	1.1618	1.942	0.23	4.8
Stvanice (Kadlíček et al., 2022)	35.8	8.5300E-01	0.199	0.844	1.689	2.026	0.23	4.9
Hochstetten sand (Khalaj, 2021)	33	1.5000E+03	0.28	0.55	0.95	1.5	0.25	1.5
Toyoura sand (Ng et al., 2013)	30	2.6000E+03	0.27	0.61	0.98	1.1	0.14	3
Firoozkuh sand (Mohammadi-Haji and Ardakani, 2020)	32.7	3.5000E+02	0.24	0.58	0.91	1.1	0.5	1
Hostun sand (Moussa et al., 2020)	32	1.0000E+03	0.29	0.61	0.96	1.9	0.13	2
Tehran silica sand (Namaei-kohal et al., 2022)	38.4	4.6000E+02	0.26	0.41	0.82	0.98	0.3	1.5
Used for model (Niemunis et al., 2005)	32.8	1.5000E+02	0.4	0.575	0.908	1.044	0.12	1

⇒

	Basic hypoplastic							
	φ_c (°)	h_s (MPa)	n	e_{d0}	e_{c0}	e_{i0}	α	β
Original model (Yang et al., 2020)	34	3.6000E+03	0.43	0.72	0.934	1.2	0.24	1.2
Karlsruhe sand (Stutz et al., 2017b)	31	1.0000E+03	0.29	0.61	0.96	1.9	0.13	2
Toyoura sand (Stutz et al., 2016)	30	2.6000E+03	0.27	0.61	0.98	1.1	0.25	1
Ticino sand (Stutz et al., 2016)	31	1.0000E+03	0.29	0.61	0.96	1.9	0.13	2
Density sand (Stutz et al., 2016)	32	7.5000E+02	0.25	0.62	0.97	1.6	0.13	1.5
Toyura sand (Stutz and Wuttke, 2018)	31	1.0000E+03	0.29	0.61	0.96	1.9	0.13	2
Berlin Sand (Le et al., 2017)	31.5	2.3000E+03	0.30	0.391	0.688	0.791	0.13	1
Castro sand (Tsegaye et al., 2010)	30.5	1.1070E+03	0.26	0.5	0.8	0.97	0.2	2
Karlsruhe fine sand (Wichtmann et al., 2019)	33.1	4.0000E+03	0.27	0.677	1.054	1.212	0.14	2.5
Kolny sand, set 1 (Mašín, 2019)	35	4.8000E+02	0.26	0.33	0.87	1.4	0.06	1.47
Kolny sand, set 2 (Mašín, 2019)	36	1.2000E+02	0.49	0.28	0.74	0.89	0.03	1.41
Parameter used (Sturm, 2009)	32.8	6.2500E+02	0.33	0.67	1.5	1.21	0.18	1.12
Toyoura sand (Arnold, 2008)	30	2.6000E+03	0.27	0.61	0.98	1.1	0.18	1

Tab 3. *Intergranular strain parameters of different types of soil*

	Intergranular strain				
	m_R	m_T	$R \times 10^{-4}$	βr	χ
Hochstetten sand (Niemunis and Herle, 1997)	5	2	1	0.5	6
Karlsruhe fine sand (Poblete et al., 2016)	5	3.5	1.4	0.35	7
Karlsruhe fine sand (Fuentes et al., 2020)	5	3.5	1.4	0.25	5
				3	17.7
Komorany sand (Mašín, 2019)	3.4	1.7	2	0.12	0.7
Toyoura sand (Ng et al., 2013)	8	4	0.2	0.1	1
Firoozkuh sand (Mohammadi-Haji and Ardakani, 2020)	5	2	1	0.5	3
Tehran silica sand (Namaei-kohal et al., 2022)	3.5	1.5	0.7	0.7	0.8
Used for model (Niemunis et al., 2005)	6.5	3	1	0.1	6
Original model (Yang et al., 2020)	1	--	3.3	0.5	3
Berlin Sand (Le et al., 2017)	4.4	2.2	1	0.2	6
Castro sand (Tsegaye et al., 2010)	5	2	1	0.5	6
Karlsruhe fine sand (Wichtmann et al., 2019)	2.2	1.1	1	0.1	5.5
Parameter used (Sturm, 2009)	6	3.5	1	0.2	6
Toyoura sand (Arnold, 2008)	5	2	1	0.12	1

3 RESULTS

3.1 Basic Parameters

3.1.1 Critical state friction angle (φc)

The critical state line (CSL) in the q-p plane was utilized to determine the value of the critical state friction angle, φ_c, using the equation:

$$q = M \times p \tag{11}$$

and the formula:

$$\sin \varphi_c = \frac{3M}{6+M} \tag{12}$$

Three monotonic triaxial tests were conducted, and the final point for each test was plotted on the q-p diagram. To obtain the M constant, a trendline was drawn, and the constant slope of the resulting linear equation 12 was designated as the M parameter.

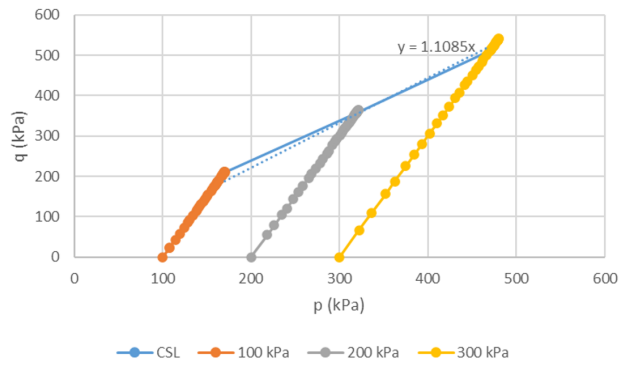


Fig. 5 *Results of triaxial tests to determine CSL*

By using equations 11 and 12, the critical state friction angle, φ_c, was computed to be 27.89289 degrees.

3.1.2 Granular hardness (hs) & Exponent (n)

It is worth mentioning that the maximum compression stress utilized in the experiment has a significant impact on granulate hardness. One might consider conducting an oedometer test on a loose sample to get these two parameters:

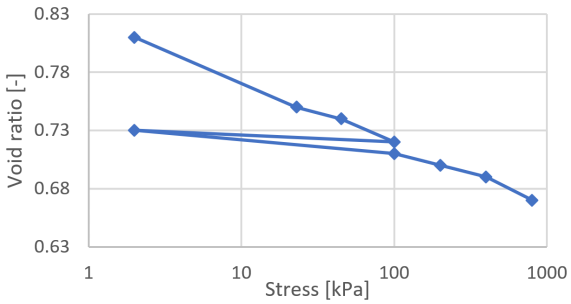


Fig. 6 *Compression Curve*

The following table is the result of the oedometer test:

Tab. 4 *Result of oedometer test*

Vertical stress (kPa)	2	100	200	400	800
Void ratio	0.73	0.71	0.7	0.69	0.67

Table 4 and equations 1 and 2 lead the parameter n and h_s as follows:

n =0.303153655

h_s =3.085316 (GPa)

3.1.3 Minimum (e_{d0}), Critical (e_{c0}) and Maximum void ratio at zero pressure (e_{i0})

The values of e_{min} and e_{max} were obtained through laboratory measurements, yielding 0.62 and 1.01, respectively. Additionally, e_{i0} was defined using the empirical formula e_{i0}=1.2*e_{c0}, which resulted in a value of 1.2 for e_{i0}. Although e_{c0} should be similar to e_{max}, previous investigations have suggested that its value is slightly lower, i.e., around 0.971. Finally, e_{min} and e_{d0} were found to be the same, with a value of 0.62 for this parameter.

3.1.4 Dilatancy (α) and Exponent (β)

In order to obtain the calibrated value for the parameters, several simulations with different values for α were performed. According to the comparison between the experimental drained cyclic triaxial test and the simulated cyclic triaxial test, the optimized value for α is 0.3. The initial void ratio for the simulated test was e_0=0.65.

β seems to mostly be independent of granulometric features, and 1 may be assumed for many natural sands.

To gain a deeper comprehension of the impact of β, multiple simulations were conducted using various values of β. The test involved 10,000 cycles, each lasting 2 seconds. The most accurate curve was identified when β was set to 1.1.

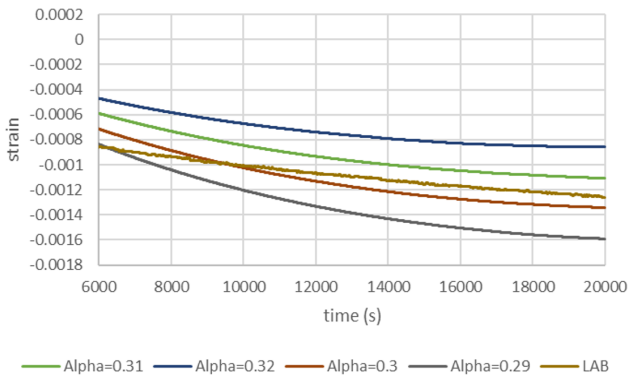


Fig. 7 *Value of the strain over time for different α's*

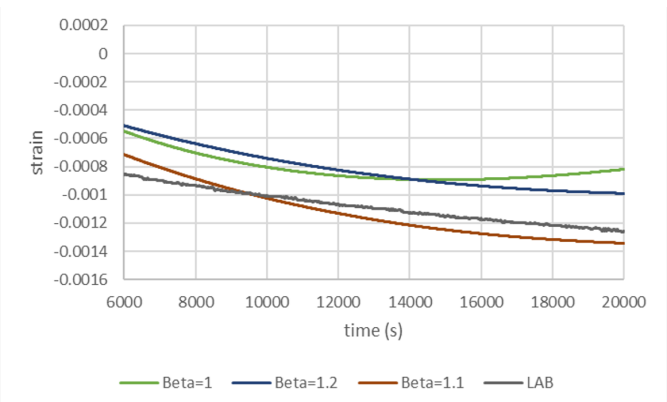


Fig. 8 *Value of the strain over time for different β's*

3.2 Intergranular parameters

3.2.1 Stiffness factor (m_R) and Parameter m_T

A comparison was conducted between the results of a drained cyclic triaxial test performed on a soil sample and a simulated triaxial test using the SoilTest Module of PLAXIS software to calibrate the intergranular strain parameters. Figure 9 shows that an increase in stiffness leads to a decrease in the amount observed of the average axial strain. According to Figure 10, setting the parameter m_T to 1 results in a similar amount of the average axial strain observed in both the simulated and laboratory samples.

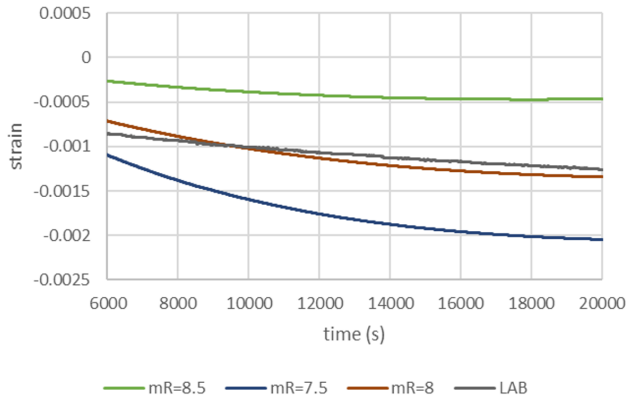


Fig. 9 *Value of the strain over time for different mR's*

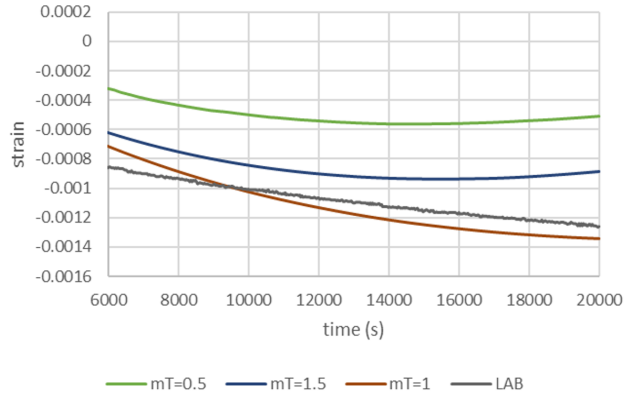


Fig. 10 *Value of the strain over time for different mT's*

3.2.2 Elastic strain amplitude, Intergranular strain hardening parameter and the exponent

According to Mašín (2019), it is difficult to differentiate the effect of m_R, β_r, and χ on the accumulation of strain caused by cyclic loading. Hence, he suggested a calibration method that involves treating $R=10^{-4}$ and $\chi=1$ as constants independent of the material. Then, m_R can be calibrated using bender element measurements, which are relatively simple to perform. Moreover, m_T can be set at $0.7*m_R$. Finally, the cyclic behavior can be controlled by adjusting only the parameter β_r.

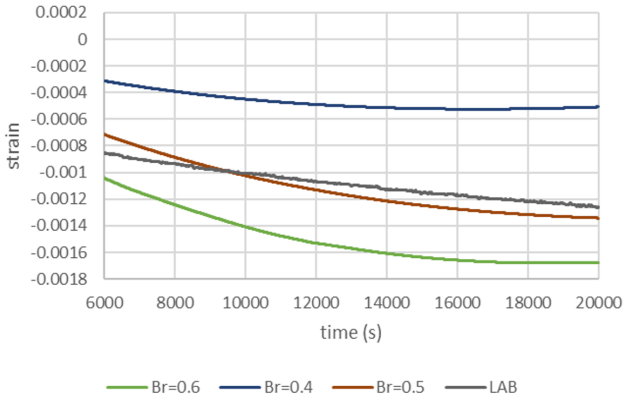


Fig. 11 *Value of the strain over time for different βr's*

Figure 12 demonstrates that increasing R_{max} alters the curvature behavior to a linear one. Furthermore, Figure 11 shows that decreasing β_r results in a reduction in the final average axial strain observed. From Figure 13, it can be inferred that the optimal value of the parameter χ is 1.2, as both higher and lower values lead to a decrease in the final average axial strain value.

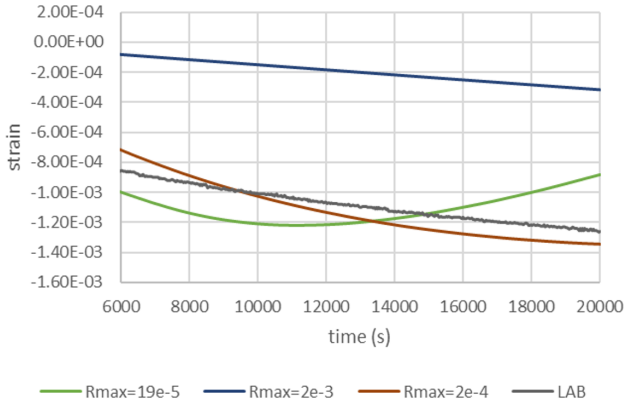


Fig. 12 *Value of the strain over time for different Rmax's*

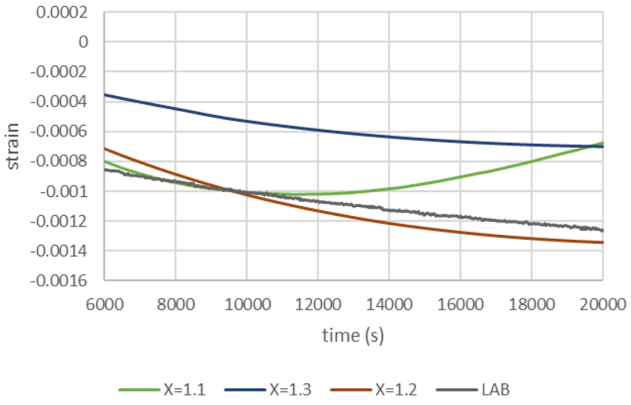


Fig. 13 *Value of the strain over time for different χ's*

4 CONCLUSIONS

This paper describes the calibration of the hypoplastic constitutive model with an intergranular strain for Danube sand using experimental static and dynamic soil tests, analytical solutions, and numerical simulations. The required parameters and their appropriate computation are provided, and the calibration technique used eliminates the need for complex geotechnical experiments. The accuracy of the constitutive parameters determined in this study was verified through numerical modeling and analytical solutions.

The values for the basic hypoplastic model parameters φ_c, n, h_s, e_{i0}, e_{d0}, e_{c0}, α, and β were determined using drained triaxial and oedometer testing, and previous research provided suggested values for e_{d0} and e_{i0}. α and β were adjusted to ensure a good fit between the simulated curve and the drained cyclic triaxial test. Similarly, the intergranular parameters m_R, m_T, β_r, R_{max}, and χ were determined through drained cyclic triaxial tests and numerical simulations to achieve the best fit.

Tab. 5 *Danube Sand data and range of basic hypoplastic parameters*

	φ_c (°)	h_s (GPa)	n	e_{d0}	e_{c0}	e_{i0}	α	β
Danube Sand	27.89	3.08	0.30	0.62	0.971	1.2	0.3	1.1
Minimum	28.6	8.53e-4	0.149	0.17	0.4	0.48	0.02	1
Maximum	42.6	32	0.56	0.844	1.689	2.026	0.5	6.3

The results show that both overestimating and underestimating χ and β lead to a lower predicted average axial strain in the final cycle. The predicted average axial strain in the first regular cycles is the same as in the experiment for all substitutional values. Thus, for long-term cyclic loading, the first cycles should not be considered. Tables 5 and 6 display the hypoplastic constitutive parameters of Danube sand, which were adjusted based on laboratory measurements. It also provides information on the range of values for each parameter, with the minimum and maximum values taken from Tables 2 and 3, which were derived from previous research.

Tab. 6 *Danube Sand data and range of intergranular strain parameters*

	m_R	m_T	R_{max}	β_r	χ
Danube Sand	8	1	2e-4	0.5	1.2
Minimum	1	1	2e-5	0.1	0.7
Maximum	8	4	3.3e-4	0.7	7

REFERENCES

Arnold, M. (2008) *Application of the intergranular strain concept to the hypoplastic modelling of non- adhesive interfaces.* 12th International Conference on Computer Methods and Advances in Geomechanics 2008, 1(1999), 747–754.

Bauer, E. – Kovtunenko, V. A. – Krejčí, P. – Krenn, N. – Sováková, L. – Zubkova, A. V. (2020) *On proportional deformation paths in hypoplasticity.* Acta Mechanica, 231(4), 1603–1619. https://doi.org/10.1007/s00707-019-02597-3

Fellin, W. (2002) *Hypoplasticity for beginners.* Institu Für Geotechnik Und Tunnelbau, (June), 1–6. Retrieved from ftp://ftp.uibk.ac.at/pub/uni-innsbruck/igt/publications/_fellin/hypo_beginner.pdf

Fu, Z. – Chen, S. – Zhong, Q. – Ji, E. (2021) *A damage hypoplasticity constitutive model for cemented sand and gravel materials.* Acta Geotechnica, *9*. https://doi.org/10.1007/s11440-021-01206-9

Fuentes, W. – Wichtmann, T. – Gil, M. – Lascarro, C. (2020) *ISA-Hypoplasticity accounting for cyclic mobility effects for liquefaction analysis.* Acta Geotechnica, 15(6), 1513–1531. https://doi.org/10.1007/s11440-019-00846-2

Gajári, G. – Kisgyörgy, L. – Ádány, S. – Mahler, A. – Lógó, J. (2021) *A visco-hypoplastic constitutive model for rolled asphalt.* Periodica Polytechnica Civil Engineering, 65(3), 798–809. https://doi.org/10.3311/PPci.17515

Herle, I. – Gudehus, G. (1999) *Determination of parameters of a hypoplastic constitutive model from properties of grain assemblies.* Mechanics of Cohesive-Frictional Materials, 4(5), 461–486. https://doi.org/10.1002/(SICI)1099-1484(199909)4:5<461::AID-CFM71>3.0.CO;2-P

Herle, I. – Kolymbas, D. (2004) *Hypoplasticity for soils with low friction angles*. Computers and Geotechnics, 31(5), 365–373. https://doi.org/10.1016/j.compgeo.2004.04.002

Kadlíček, T. – Janda, T. – Šejnoha, M. (2016) *Calibration of Hypoplastic Models for Soils.* Applied Mechanics and Materials, 821, 503–511. https://doi.org/10.4028/www.scientific. net/amm.821.503

Kadlíček, T. – Janda, T. – Šejnoha, M. – Mašín, D. – Najser, J. – Beneš, Š. (2022) Automated calibration of advanced soil constitutive models. Part I: hypoplastic sand. Acta Geotechnica,17(8), 3421–3438. https://doi.org/10.1007/s11440-021-01441-0

Khalaj, O. – Abedin Nejad, S. – Janda, T. (2021) *Multi Elements Simulation of Biaxial Test with Two Different Soil Layers Using Hypoplastic Constitutive Model.* IOP Conference Series: Materials Science and Engineering, 1161(1), 012001. https://doi.org/10.1088/1757-899x/1161/1/012001

Kolymbas, D. – Wu, W. (1990) *Recent results of triaxial tests with granular materials.* Powder Technology, 60(2), 99–119. https://doi.org/10.1016/0032-5910(90)80136-M

Le, V. H. – Rackwitz, F. – Savidis, S. A. (2017) *Accumulation of monopile deformation in sand due to change in load direction.* (March 2018).

Mašín, D. (2019) *Modelling of Soil Behaviour with Hypoplasticity: Another Approach to Soil Constitutive Modelling.*

Mašín, D. (2015) *Hypoplasticity for Practical Applications Part 4: Determination of material parameters*.

Mohammadi-Haji, B. – Ardakani, A. (2020) *Calibration of a Hypoplastic Constitutive Model with Elastic Strain Range for Firoozkuh Sand.* Geotechnical and Geological Engineering, 38(5), 5279– 5293. https://doi.org/10.1007/s10706-020-01363-w

Moussa, A. – Salah, M. – Rafik, D. (2020) *Improvement of a Hypoplastic Model for Granular Materials Under High-Confining Pressures.* Geotechnical and Geological Engineering, 38(4), 3761–3771. https://doi.org/10.1007/s10706-020-01256-y

Namaei-kohal, A. – Ardakani, A. – Hassanlourad, M. (2022) *Hypoplastic soil model parameters calibration for Tehran silica sand and verification with a monotonic geocell pullout test.* Arabian Journal of Geosciences, 15(9). https://doi.org/10.1007/s12517-022-10110-9

Ng, Ch. W. W. – Boonyarak, T. – Mašín, D. (2013) *Three-dimensional centrifuge and numerical modeling of the interaction between perpendicularly crossing tunnels.* Canadian Geotechnical Journal, 50(9), 935–946. https://doi.org/10.1139/cgj-2012-0445

Niemunis, A. – Herle, I. (1997) *Hypoplastic model for cohesionless soils with elastic strain range.* Mechanics of Cohesive-Frictional Materials, 2(4), 279–299. https://doi.org/10.1002/(SICI)1099-1484(199710)2:4<279::AID-CFM29>3.0.CO; 2-8

Niemunis, A. – Wichtmann, T. – Triantafyllidis, T. (2005) *A high-cycle accumulation model for sand.* Computers and Geotechnics, 32(4), 245–263. https://doi.org/10.1016/j.compgeo.2005.03.002

Poblete, M. – Fuentes, W. – Triantafyllidis, T. (2016) *On the simulation of multidimensional cyclic loading with intergranular strain.* Acta Geotechnica, 11(6), 1263–1285. https://doi.org/10.1007/s11440-016-0492-2

Sturm, H. (2009) *Numerical investigation of the stabilisation behaviour of shallow foundations under alternate loading.* Acta Geotechnica, 4(4), 283–292. https://doi.org/10.1007/s11440-009-0102-7

Stutz, H. H. – Wuttke, F. (2018) *Hypoplasticmodeling of soil-structure interfaces in offshore applications.* Journal of Zhejiang University: Science A, 19(8), 624–637. https://doi.org/10.1631/jzus.A1700469

Stutz, H. – Mašín, D. – Sattari, A. S. – Wuttke, F. (2017a) *A general approach to model interfaces using existing soil constitutive models application to hypoplasticity*. Computers and Geotechnics, 87, 115–127. https://doi.org/10.1016/j.compgeo.2017.02.010

Stutz, H. – Mašín, D. – Sattari, A. S. – Wuttke, F. (2017b) *A general approach to model interfaces using existing soil constitutive models application to hypoplasticity.* Computers and Geotechnics, 87, 115–127. https://doi.org/10.1016/j.compgeo.2017.02.010

Stutz, H. – Mašín, D. – Wuttke, F. (2016) *Enhancement of a hypoplastic model for granular soil–structure interface behaviour.* Acta Geotechnica, 11(6), 1249–1261. https://doi.org/10.1007/s11440-016-0440-1

Tsegaye, A. B. – Molenkamp, F. – Brinkgreve, R. B. J. – Bonnier, P. G. – De Jager, R. – Galavi, V. (2010) *Modeling liquefaction behavior of sands by means of hypoplastic model.* Numerical Methods in Geotechnical Engineering - Proceedings of the 7th European Conference on Numerical Methods in Geotechnical Engineering, (1), 81–87. https://doi.org/10.1201/b10551-18

von Wolffersdorff, P. A. (1996) *Hypoplastic relation for granular materials with a predefined limit state surface.* Mechanics of Cohesive-Frictional Materials, 1(3), 251–271. https://doi.org/10.1002/(SICI)1099-1484(199607)1:3<251::AID-CFM13>3.0.CO;2-3

Wang, S. – Wu, W. (2020) *A simple hypoplastic model for overconsolidated clays.* Acta Geotechnica, 16(1), 21–29. https://doi.org/10.1007/s11440-020-01000-z

Wei, X. – Chen, Y. – Yang, J. (2020) *A unified critical state constitutive model for cyclic behavior of silty sands.* Computers and Geotechnics, 127 (July), 103760. https://doi.org/10.1016/j.compgeo.2020.103760

Wichtmann, T. – Fuentes, W. – Triantafyllidis, T. (2019) *Inspection of three sophisticated constitutive models based on monotonic and cyclic tests on fine sand: Hypoplasticity vs. Sanisand vs. ISA.* Soil Dynamics and Earthquake Engineering, 124 (April 2018), 172–183. https://doi.org/10.1016/j.soildyn.2019.05.001

Wichtmann, T. – Triantafyllidis, T. (2018) *Monotonic and cyclic tests on kaolin: a database for the development, calibration and verification of constitutive models for cohesive soils with focus to cyclic loading.* Acta Geotechnica, 13(5), 1103–1128. https://doi.org/10.1007/s11440-017-0588-3

Wu, W. – Bauer, E. (1994) *A simple hypoplastic constitutive model for sand*. International Journal for Numerical and Analytical Methods in Geomechanics, 18(12), 833–862. https://doi.org/10.1002/nag.1610181203

Wu, W. – Lin, J. – Wang, X. (2017) *A basic hypoplastic constitutive model for sand.* Acta Geotechnica, 12(6), 1373–1382. https://doi.org/10.1007/s11440-017-0550-4

Yang, Z. – Liao, D. – Xu, T. (2020) *A hypoplastic model for granular soils incorporating anisotropic critical state theory.* International Journal for Numerical and Analytical Methods in Geomechanics, 44(6), 723–748. https://doi.org/10.1002/nag.3025